Clinical Interventions in Aging

Dovepress
Taylor & Francis Group

Open Access Full Text Article

ORIGINAL RESEARCH

Host Susceptibility Phenotypes and Construction of an Inflammation–Vascular–Metabolic (IVM) Integrated Score for Hard-to-Heal Wounds After Low-Energy Foot Trauma in Older Adults

Lijun Xiu[1], Tiantian Liu[2], Zhaoxia Ji[1], Xinzhe Zhang[1], Guanghai Yuan[1], Jian Li[1], Peng Yang[1]

[1]Department of Hand and Foot Surgery, Qingdao Eighth People's Hospital, Qingdao, Shandong, 266100, People's Republic of China; [2]Department of Ophthalmology, Qingdao Eighth People's Hospital, Qingdao, Shandong, 266100, People's Republic of China

Correspondence: Peng Yang, Department of Hand and Foot Surgery, Qingdao Eighth People's Hospital, 84 Fengshan Road, Licang District, Qingdao, Shandong, 266100, People's Republic of China, Email yangpengsd00@163.com

Background: Older adults with low-energy trauma-initiated foot wounds often become hard-to-heal, but prognostic tools tailored to this scenario are scarce.

Methods: In this single-center retrospective cohort, we included consecutive patients aged ≥65 years with below-malleoli low-energy trauma-initiated foot wounds. Baseline predictors were the first laboratory values within 48 h and an ordinal perfusion/ischemia category derived from available ABI, pedal Doppler waveform findings, and toe-based measures. Hard-to-heal was failure of complete epithelialization without drainage by 12 weeks (major amputation classified as not healed). Latent class analysis defined susceptibility phenotypes. An interpretable 6-variable inflammation–vascular–metabolic (IVM) model was developed using logistic regression with multiple imputation and bootstrap internal validation.

Results: Among 697 patients (median age 74 years), 332 (47.6%) were hard-to-heal at 12 weeks. Phenotypes showed graded risk (lowest to highest): relatively resilient (n=143, hard-to-heal 26/143), renal-hypoalbuminemia (n=165, hard-to-heal 81/165), metabolic–inflammatory (n=206, hard-to-heal 110/206), and ischemia-dominant (n=183, hard-to-heal 115/183). Adjusted odds ratios versus resilient were 3.8 (95% CI 2.3–6.4), 4.5 (2.8–7.4), and 6.1 (3.7–10.1), respectively. The IVM model achieved optimism-corrected AUC 0.80 (95% CI 0.77–0.83) with calibration slope 0.94 (intercept −0.03), stratified observed event rates to 19.7% (50/254), 48.8% (137/281), and 89.5% (145/162), and showed net benefit across threshold probabilities ~0.25–0.70.

Conclusion: In this retrospective single-center cohort, distinct susceptibility phenotypes were identifiable and the IVM score provided internally validated early risk stratification. External validation and prospective evaluation are warranted before routine clinical implementation.

Keywords: wound healing, older adults, low-energy trauma, perfusion, inflammation, latent class analysis, risk prediction

Introduction

Chronic nonhealing wounds impose a substantial clinical and economic burden in aging societies, with large-scale payer data demonstrating that wound-related care accounts for major healthcare expenditures across multiple wound categories.[1] In parallel, low-energy falls are highly prevalent among adults aged ≥65 years and represent a leading cause of injury, creating frequent opportunities for seemingly minor foot trauma to become a persistent wound in vulnerable hosts.[2] Low-energy foot trauma may appear superficially minor, yet in older adults it can unmask impaired host repair capacity, perfusion limitation, or metabolic vulnerability that is less visible at the initial wound assessment.[2,3] Aging further increases risk because cutaneous repair becomes dysregulated, with delayed resolution of inflammation and increased oxidative stress that can shift healing toward chronicity even after limited tissue damage.[3] Real-world wound outcomes are also highly heterogeneous and can be misleading without appropriate risk adjustment, highlighting why

https://doi.org/10.2147/CIA.S604608
Received: 22 February 2026
Accepted: 26 May 2026
Published: 30 June 2026

context-specific prognostic approaches are needed when comparing healing rates or guiding escalation pathways.[4] However, much of the existing risk-prediction literature and triage logic has been developed in diabetic foot ulcer (DFU) or mixed-etiology cohorts, and systematic appraisal has identified frequent methodological limitations and limited validation.[5] Mixed-etiology electronic health record models have also shown that 12-week healing prediction is feasible, but such models combine venous, arterial, pressure, diabetic, and other wound types, leaving uncertainty about transportability to geriatric trauma-initiated foot wounds.[6]

From an immunological perspective, successful wound healing requires a coordinated progression through hemostasis, inflammation, proliferation, and remodeling, driven by tightly regulated interactions between stromal cells, endothelial cells, and recruited leukocytes.[7] Early innate immune responses are essential for microbial control and clearance of damaged tissue, but must transition toward pro-repair programs (including macrophage phenotypic switching and resolution pathways) to enable angiogenesis, extracellular matrix deposition, and re-epithelialization.[8] When this inflammatory-to-proliferative transition fails, wounds can become chronic, characterized by persistent leukocyte-driven inflammation, excessive protease activity, and impaired matrix formation and tissue restoration.[9] Importantly, modern human wound biology emphasizes marked cellular heterogeneity and context-dependent immune–stromal crosstalk, implying that clinically similar wounds may follow different trajectories because they arise from distinct underlying immune states.[10] Consistent with this framework, mechanistic insight into pathological healing supports the need to capture host-level immune dysregulation when developing clinically actionable risk stratification.[11]

Perfusion is a key upstream determinant of both antimicrobial defense and tissue reconstruction because oxygen and nutrient delivery are required for oxidative killing, collagen synthesis, angiogenic signaling, and efficient trafficking of immune cells into injured tissue, and guideline-based approaches therefore emphasize objective vascular assessment when foot wounds are slow to progress.[12] Toe systolic pressure provides complementary information to ABI, and meta-analytic evidence supports its utility for estimating healing potential and guiding escalation of vascular evaluation and limb-salvage planning.[13] Beyond perfusion, the metabolic–nutrition–immune axis (immunometabolism) is central to wound outcomes, as hyperglycemia during acute illness or chronic disease states can dysregulate innate immunity and host defense, thereby increasing susceptibility to infection and impairing organized repair.[14] Malnutrition and hypoalbuminemia further compromise immune competence and substrate availability for granulation and remodeling, and are consistently linked to delayed healing and higher complication risk in complex wounds.[15] Chronic kidney disease compounds these vulnerabilities through combined immune dysfunction and inflammatory amplification, reinforcing the rationale for an integrated inflammation–vascular–metabolic framework and an interpretable early IVM risk score in older adults with low-energy trauma-initiated foot wounds.[16]

In our study, we prespecified two complementary objectives in older adults presenting with low-energy trauma-initiated foot wounds below the malleoli. "Hard-to-heal" was used operationally to mean failure of complete epithelialization without drainage by 12 weeks after the index assessment. First, we aimed to identify host susceptibility phenotypes defined by separable patterns across inflammatory/immune-balance markers, distal perfusion impairment, and metabolic–nutritional/organ-reserve features, and to quantify their independent associations with 12-week hard-to-heal outcomes. Second, we aimed to develop and internally validate a parsimonious, clinically implementable six-variable inflammation–vascular–metabolic (IVM) score using routine data available at the index assessment (lnCRP, neutrophil-to-lymphocyte ratio, perfusion category, glucose, albumin, and eGFR).

Methods

Study Design and Data Source

This was a single-center retrospective cohort study conducted at the Qingdao Eighth People's Hospital that aimed to (1) identify host susceptibility phenotypes among older adults with low-energy trauma-initiated foot wounds and (2) develop and internally validate an interpretable inflammation–vascular–metabolic (IVM) model for predicting 12-week non-healing. Consecutive eligible patients between January 1, 2018 and December 31, 2024 were identified through the electronic medical record and wound-care documentation systems, and the index assessment was defined as the first qualifying evaluation at our institution for the trauma-initiated wound. This study was conducted in accordance with the

Declaration of Helsinki. The protocol was reviewed and approved by the Ethics Committee of the Qingdao Eighth People's Hospital (QBYLLKY2026012), which waived the requirement for informed consent because this was a retrospective analysis of de-identified routinely collected data and posed no more than minimal risk to participants. All data were anonymized prior to analysis.

Participants

Patients were eligible if they were aged ≥65 years and had a trauma-initiated wound/ulcer located below the malleoli attributed to a low-energy mechanism (eg., fall from standing height, minor blunt injury, or friction injury). High-energy trauma mechanisms and wounds clearly documented as primarily non-traumatic etiologies (eg., vasculitic or malignancy-associated ulcers) were excluded when ascertainable from the record. To maintain one observation per participant, when multiple wounds were present, a single index wound was prespecified as the clinically dominant wound at presentation (largest area or deepest tissue involvement based on documentation). Eligibility required sufficient documentation to adjudicate the 12-week outcome.

Outcome Definition and Ascertainment

The primary outcome was 12-week non-healing (operationally defined as "hard-to-heal"), defined as failure to achieve complete epithelialization without drainage by 12 weeks after the index assessment; major amputation during follow-up was classified as not healed for the primary endpoint. Outcome ascertainment was performed using structured wound clinic notes, inpatient records, and procedural documentation. When serial assessments were available, the earliest date meeting complete epithelialization criteria was used to classify healing within the 12-week window. When documentation was insufficient to confirm healing status within 12 weeks, the case was excluded from the analytic cohort.

Baseline Clinical Assessment, Comorbidities, and Wound Characteristics

Baseline variables were abstracted from index assessment documentation and the medical history, including age, sex, diabetes mellitus, peripheral artery disease (PAD), chronic kidney disease (CKD), current smoking status, and clinical infection at presentation. Clinical infection at presentation was operationalized as a binary variable (present/absent) based on clinician documentation of infection and/or explicitly documented local/systemic inflammatory features (eg., erythema, warmth, swelling/induration, pain/tenderness, purulent drainage, fever), recognizing that antibiotic initiation alone is not a stand-alone diagnostic criterion. Wound size was recorded as wound area (cm^2) based on routine clinical measurement documented at presentation.

Perfusion Evaluation and Perfusion Category Construction

Arterial perfusion was assessed using objective tests available in routine care, including ankle–brachial index (ABI), pedal Doppler waveforms, and toe-based measures (toe systolic pressure and/or toe–brachial index) when available. Because testing was not uniform across patients, perfusion status was summarized using a prespecified hierarchical and clinically interpretable ordinal perfusion/ischemia category with four levels, adequate, borderline, moderate ischemia, and severe ischemia or noncompressible ABI, where the highest category captured either markedly impaired perfusion or noncompressible ABI (a measurement limitation that indicates toe-based assessment is required to better estimate distal perfusion and healing likelihood). Perfusion categories were assigned hierarchically using the most distal available hemodynamic information (toe systolic pressure/TBI preferred, then ABI, then pedal Doppler waveform), applying the worst (most ischemic) result when multiple tests were available. Cutoffs were prespecified and aligned with PAD/CLTI guidance: adequate (toe systolic pressure ≥60 mmHg or TBI ≥0.70, or ABI 0.90–1.30 with multiphasic Doppler); borderline (toe 40–59 mmHg or TBI 0.50–0.69, or ABI 0.70–0.89 or biphasic Doppler); moderate ischemia (toe 30–39 mmHg or TBI 0.30–0.49, or ABI 0.50–0.69 or monophasic Doppler); severe ischemia/noncompressible (toe <30 mmHg or TBI <0.30, or ABI <0.50; ABI >1.30 was considered noncompressible and classified as noncompressible unless toe-based measures were available, in which case toe-based cutoffs were used).

Laboratory Assays and Derived Biomarkers

Baseline laboratory predictors were defined as the first available results obtained within 48 hours of the index assessment, including C-reactive protein (CRP, mg/L), complete blood count, serum glucose (mmol/L), albumin (g/L), creatinine-derived estimated glomerular filtration rate (eGFR, mL/min/1.73m^2), and hemoglobin (g/L). The neutrophil-to-lymphocyte ratio (NLR) was calculated as the absolute neutrophil count divided by the absolute lymphocyte count from the same blood draw. For modeling, CRP was natural log-transformed (ln[CRP in mg/L]) to address right-skewness and improve model fit, while CRP was summarized in tables on the original scale for clinical interpretability. Index glucose was taken from the same draw. eGFR was computed using the laboratory-reported equation used in routine care at our institution.

Host Susceptibility Phenotypes

Host susceptibility phenotypes were derived using latent class analysis (finite mixture modeling with mixed indicators) incorporating baseline inflammatory and immune-balance surrogates (lnCRP and NLR), vascular status (ordinal perfusion/ischemia category), and metabolic–nutritional/organ-reserve markers (glucose, albumin, eGFR). Models with two to five classes were fitted using multiple random starts; continuous indicators were standardized for class generation and ordinal perfusion category was modeled as an ordered indicator. The number of classes was selected by considering information criteria (AIC/BIC), entropy, class sizes, and clinical interpretability. Outcome status was not used to derive the latent classes. Phenotype labels were assigned based on dominant feature patterns. Phenotype profiles were summarized using clinically interpretable distributions and visualized as standardized z-scores across key domains.

Phenotype–Outcome Association Modeling

Associations between phenotypes and the 12-week hard-to-heal outcome were estimated using logistic regression with the relatively resilient phenotype as the reference. A prespecified adjusted model included age, sex, diabetes mellitus, wound area, and clinical infection at presentation as baseline covariates chosen a priori to capture demographics, baseline wound burden, and infection/metabolic context. Unadjusted and adjusted odds ratios (ORs) with 95% confidence intervals (CIs) were reported.

IVM Model Development, Internal Validation, and Risk Stratification

The IVM model was specified a priori to include six routinely available predictors representing inflammation–vascular–metabolic domains: ln(CRP), NLR, ordinal perfusion/ischemia category, glucose, albumin, and eGFR. These predictors were selected before outcome modeling to preserve interpretability, maintain an adequate events-per-variable ratio, and avoid overfitting; no automated variable selection was performed. Logistic regression was used for the prediction model. eGFR was scaled per 10 mL/min/1.73m^2 for interpretability. Model discrimination was quantified using the area under the ROC curve, calibration was assessed using a decile-based calibration plot and calibration intercept/slope derived from regressing outcome on the logit of predicted risk, and clinical utility was evaluated using decision curve analysis. Internal validation used bootstrap resampling to estimate optimism in performance metrics and to obtain robust uncertainty estimates. Bootstrap validation used 1,000 resamples.

Predicted risks were categorized into three clinically interpretable strata using two probability thresholds (low <0.25; intermediate 0.25–0.70; high >0.70) and stratum-specific observed event rates with 95% CIs were reported.

Statistical Analysis

Continuous variables were summarized as median [IQR] and compared using Mann–Whitney *U*-tests (two-group comparisons) or Kruskal–Wallis tests (four phenotype groups), while categorical variables were summarized as n (%) and compared using χ^2 tests (or Fisher's exact tests where appropriate). Because multiple descriptive comparisons were reported in baseline and phenotype profiling tables, univariable p values were provided for description and were not used as the primary basis for inference; interpretation focuses on prespecified multivariable models and prediction

performance. All tests were two-sided with a nominal alpha of 0.05. Analyses were performed using R (Version 4.3, R Foundation for Statistical Computing, Vienna, Austria).

Multiple imputation by chained equations (20 imputed datasets, 20 iterations) was used to handle missing predictor data for multivariable modeling under a missing-at-random assumption. Imputation models included the outcome, all candidate predictors, phenotype indicators, and auxiliary baseline variables. Estimates were pooled using Rubin's rules. Missingness for variables used in multivariable modeling was low (0.0%–5.9% across laboratory and clinical predictors). A complete-case sensitivity analysis was performed for the main phenotype associations and IVM discrimination.

Results

Study Cohort and Baseline Characteristics

Screening began with 823 potentially eligible records; 126 were excluded (high-energy mechanism, n=29; primary non-traumatic etiology, n=31; duplicate/non-index wound episode, n=24; insufficient 12-week outcome documentation, n=42), yielding 697 older adults with low-energy trauma-initiated foot wounds, of whom 332 (47.6%) met the primary endpoint of 12-week non-healing (hard-to-heal) and 365 (52.4%) healed within 12 weeks (Figure 1 and Table 1). Median age was 74.4 years (IQR 69.7–79.5), and the hard-to-heal group was modestly older than the healed group (75.1 [70.7–80.4] vs 74.0 [68.8–78.6] years; p=0.005) (Table 1). PAD and CKD were more prevalent among hard-to-heal patients (PAD 45.8% vs 37.0%, p=0.018; CKD 29.2% vs 22.2%, p=0.034), while diabetes prevalence and smoking status were similar between outcome groups (Table 1). Clinical infection at presentation was more frequent in hard-to-heal patients (34.0% vs 27.1%; p=0.048) (Table 1). Perfusion status differed substantially by outcome, with the hard-to-heal group showing a marked shift toward worse perfusion categories and a higher proportion classified as severe ischemia or noncompressible ABI (31.0% vs 12.9%), and the overall perfusion category distribution differed significantly (overall p<0.001) (Table 1). Inflammatory and immunometabolic biomarkers also differed, with higher CRP, NLR, and glucose in the hard-to-heal group and lower albumin, eGFR, and hemoglobin, each differing in univariable comparisons (Table 1).

Host Susceptibility Phenotypes

Latent class analysis identified four clinically interpretable host susceptibility phenotypes with distinct inflammatory, vascular, and metabolic–nutritional patterns (Table 2 and Figure 2). The four-class solution was selected over two-, three-

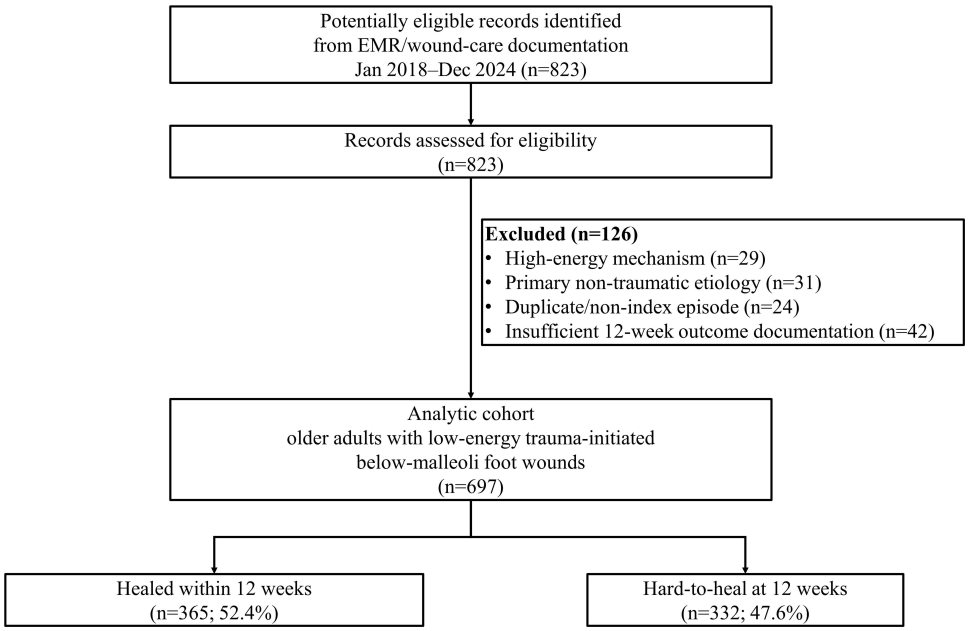

Figure 1 Study flow diagram. Flow diagram summarizing record screening, exclusions, analytic cohort formation, and 12-week outcome groups. The final analytic cohort included 697 older adults with low-energy trauma-initiated foot wounds; 365 healed and 332 were hard-to-heal by 12 weeks.

https://doi.org/10.2147/CIA.S604608

Table 1 Baseline Characteristics (Overall and by 12-Week Outcome)

Characteristic	Overall (n=697)	Healed (n=365)	Hard-to-Heal (n=332)	*p* Value
Male, n (%)	407 (58.4)	210 (57.5)	197 (59.3)	0.630
Diabetes mellitus, n (%)	279 (40.0)	144 (39.5)	135 (40.7)	0.745
Peripheral artery disease (PAD), n (%)	287 (41.2)	135 (37.0)	152 (45.8)	0.018
Chronic kidney disease (CKD), n (%)	178 (25.5)	81 (22.2)	97 (29.2)	0.034
Current smoker, n (%)	123 (17.6)	62 (17.0)	61 (18.4)	0.631
Clinical infection at presentation, n (%)	212 (30.4)	99 (27.1)	113 (34.0)	0.048
Perfusion category, n (%)				<0.001
Adequate	161 (23.1)	115 (31.5)	46 (13.9)	
Borderline	200 (28.7)	107 (29.3)	93 (28.0)	
Moderate ischemia	186 (26.7)	96 (26.3)	90 (27.1)	
Severe/noncompressible	150 (21.5)	47 (12.9)	103 (31.0)	
Age (years), median [IQR]	74.4 [69.7–79.5]	74.0 [68.8–78.6]	75.1 [70.7–80.4]	0.005
Wound area (cm^2), median [IQR]	0.98 [0.64–1.53]	0.94 [0.60–1.51]	1.04 [0.66–1.58]	0.177
CRP (mg/L), median [IQR]	20.1 [11.3–33.5]	16.1 [8.8–26.2]	25.5 [15.8–42.1]	<0.001
NLR, median [IQR]	4.9 [3.7–6.6]	4.3 [3.3–5.6]	5.9 [4.4–7.4]	<0.001
Glucose (mmol/L), median [IQR]	7.3 [5.8–8.8]	6.9 [5.3–8.4]	7.8 [6.5–9.2]	<0.001
Albumin (g/L), median [IQR]	35.9 [33.2–38.8]	37.4 [34.3–40.2]	34.5 [32.0–37.1]	<0.001
eGFR (mL/min/1.73m^2), median [IQR]	65.4 [52.5–77.9]	69.1 [55.9–80.9]	61.1 [49.8–74.7]	<0.001
Hemoglobin (g/L), median [IQR]	126.0 [114.4–136.1]	127.3 [116.2–137.8]	124.0 [113.0–135.3]	0.010

Table 2 Host Susceptibility Phenotypes: Clinical/Biologic Profile

Variable	Ischemia-Dominant (n=183)	Metabolic–Inflammatory (n=206)	Renal–Hypoalbuminemia (n=165)	Relatively Resilient (n=143)	*p* Value
Hard-to-heal at 12 weeks, n (%)	115 (62.8)	110 (53.4)	81 (49.1)	26 (18.2)	—
Age (years), median [IQR]	76.0 [70.3–80.7]	74.4 [69.5–79.5]	76.5 [72.7–83.8]	71.2 [66.9–74.6]	<0.001
Male (%)	63.4	63.1	43.6	62.2	<0.001
Diabetes mellitus, %	42.6	53.9	33.9	23.8	<0.001
Peripheral artery disease (PAD), %	67.8	33.0	43.0	16.8	<0.001
Chronic kidney disease (CKD), %	32.2	23.3	35.2	9.1	<0.001
Moderate-to-severe ischemia (PerfCat≥2), %	74.3	48.1	46.1	17.5	<0.001
CRP (mg/L), median [IQR]	20.6 [13.6–30.6]	33.3 [22.5–51.4]	19.3 [11.7–29.5]	8.8 [5.7–12.9]	<0.001
NLR, median [IQR]	6.4 [5.2–8.1]	5.3 [3.9–6.8]	4.6 [3.6–6.0]	3.4 [2.7–4.4]	<0.001
Glucose (mmol/L), median [IQR]	7.2 [6.0–8.5]	8.6 [7.2–10.1]	6.8 [5.6–8.2]	5.8 [4.6–7.5]	<0.001
Albumin (g/L), median [IQR]	35.7 [32.7–37.9]	36.8 [34.5–39.5]	33.2 [31.0–35.3]	38.8 [36.0–41.5]	<0.001
eGFR, mL/min/1.73m^2, median [IQR]	64.0 [52.5–74.6]	69.9 [58.8–81.0]	53.0 [44.2–62.8]	78.0 [67.8–87.5]	<0.001

https://doi.org/10.2147/CIA.S604608

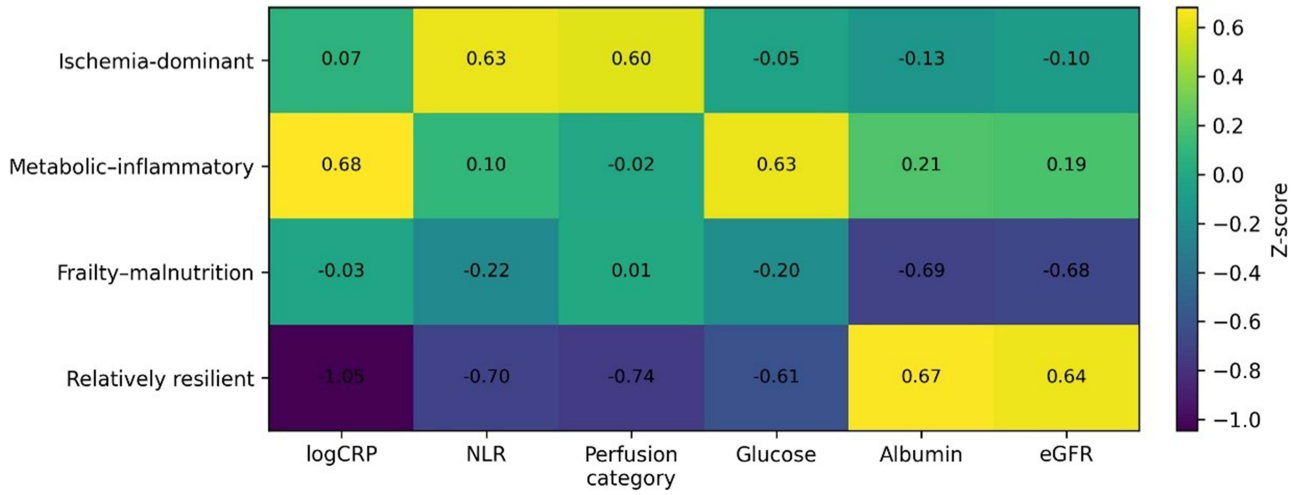

Figure 2 Phenotype heatmap. Heatmap showing phenotype-specific mean z-score for the six IVM indicator domains (ln(CRP), NLR, ordinal perfusion category, glucose, albumin, and eGFR). Higher values indicate a higher phenotype-specific mean relative to the overall cohort, except albumin and eGFR where lower z-scores indicate lower reserve.

, and five-class alternatives because it provided a favorable balance of fit and stability (AIC 5821.4; BIC 5982.7; entropy 0.81; minimum class size 143 [20.5%]). The ischemia-dominant phenotype (n=183) showed the highest PAD burden (67.8%) and the most adverse perfusion pattern (greater proportion with moderate-to-severe ischemia), the metabolic–inflammatory phenotype (n=206) had the highest diabetes prevalence (53.9%) and biomarker patterns consistent with heightened inflammation and hyperglycemia, and the renal-hypoalbuminemia phenotype (n=165) demonstrated the highest CKD prevalence (35.2%) and a profile characterized by lower eGFR and lower albumin (an integrated marker of inflammation/catabolism) (Table 2). The relatively resilient phenotype (n=143) was younger and exhibited lower comorbidity burden and more favorable perfusion and biomarker patterns, consistent with its label (Table 2 and Figure 2). Across phenotypes, differences in non-indicator variables (eg., age and comorbidities) are summarized in Table 2. The six indicator variables used to derive the latent classes were presented descriptively.

Phenotype Associations with 12-Week Hard-to-Heal Outcome

Hard-to-heal event rates differed markedly across phenotypes, ranging from 18.2% (26/143) in the relatively resilient phenotype to 49.1% (81/165) in renal-hypoalbuminemia, 53.4% (110/206) in metabolic–inflammatory, and 62.8% (115/183) in ischemia-dominant (Table 2). Using relatively resilient as the reference group, unadjusted odds of hard-to-heal were substantially higher in the vulnerable phenotypes (ischemia-dominant OR 7.6 [95% CI 4.5–12.8], metabolic–inflammatory OR 5.2 [3.1–8.5], and renal-hypoalbuminemia OR 4.3 [2.6–7.3]; all $p<0.001$) (Table 3). After adjustment for prespecified baseline covariates (age, sex, diabetes mellitus, wound area, and clinical infection), phenotype associations remained strong and directionally consistent, with adjusted ORs of 6.1 (95% CI 3.7–10.1) for ischemia-dominant, 4.5 (2.8–7.4) for metabolic–inflammatory, and 3.8 (2.3–6.4) for renal-hypoalbuminemia compared with the relatively resilient phenotype (Table 3).

Table 3 Phenotypes and 12-Week Hard-to-Heal Outcome

Phenotype (Ref: Relatively Resilient)	Unadjusted OR (95% CI)	*p* Value	Adjusted OR (95% CI)	Adj. *p* Value
Ischemia-dominant	7.6 (4.5–12.8)	<0.001	6.1 (3.7–10.1)	<0.001
Metabolic–inflammatory	5.2 (3.1–8.5)	<0.001	4.5 (2.8–7.4)	<0.001
Renal–hypoalbuminemia	4.3 (2.6–7.3)	<0.001	3.8 (2.3–6.4)	<0.001

https://doi.org/10.2147/CIA.S604608

Table 4 IVM Model: Predictors and Risk Strata

A. IVM model coefficients			
Predictor	**Beta**	**OR (95% CI)**	***p* value**
ln (CRP) per 1 unit	0.748	2.11 (1.63–2.73)	<0.001
NLR per 1 unit	0.261	1.30 (1.19–1.42)	<0.001
Perfusion category per 1 level	0.319	1.38 (1.16–1.63)	<0.001
Glucose (mmol/L) per 1 unit	0.101	1.11 (1.02–1.20)	0.018
Albumin (g/L) per 1 unit	−0.146	0.86 (0.82–0.91)	<0.001
eGFR per 10 mL/min/1.73m^2	−0.111	0.89 (0.81–0.99)	0.029
B. Three-tier risk stratification			
Risk stratum	**n**	**Hard-to-heal, n (%)**	**95% CI, %**
Low (<0.25)	254	50 (19.7)	15.3–25.0
Intermediate (0.25–0.70)	281	137 (48.8)	43.0–54.6
High (>0.70)	162	145 (89.5)	83.8–93.3

IVM Model Coefficients and Discrimination, Calibration, and Clinical Utility

In the six-variable IVM model, higher ln(CRP), higher NLR, worse perfusion category, and higher glucose were associated with increased odds of hard-to-heal, whereas higher albumin and higher eGFR were associated with reduced odds (Table 4A). Discrimination was good, with an optimism-corrected AUC of 0.80 (95% CI 0.77–0.83) (Figure 3). Calibration was strong with calibration slope 0.94 and intercept −0.03 (Figure 4). Decision curve analysis suggested that

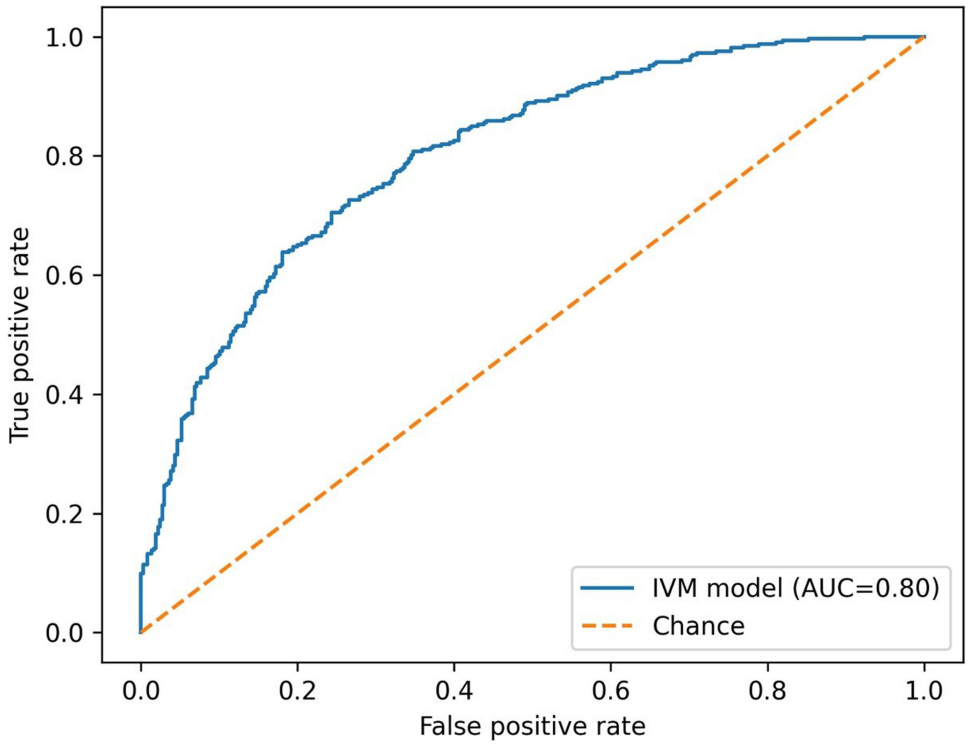

Figure 3 Receiver operating characteristic (ROC) curve for the IVM model. ROC curve for the internally validated six-variable IVM logistic model predicting 12-week hard-to-heal outcome. The diagonal dashed line represents chance discrimination; the optimism-corrected AUC was 0.80 (95% CI 0.77–0.83).

 https://doi.org/10.2147/CIA.S604608

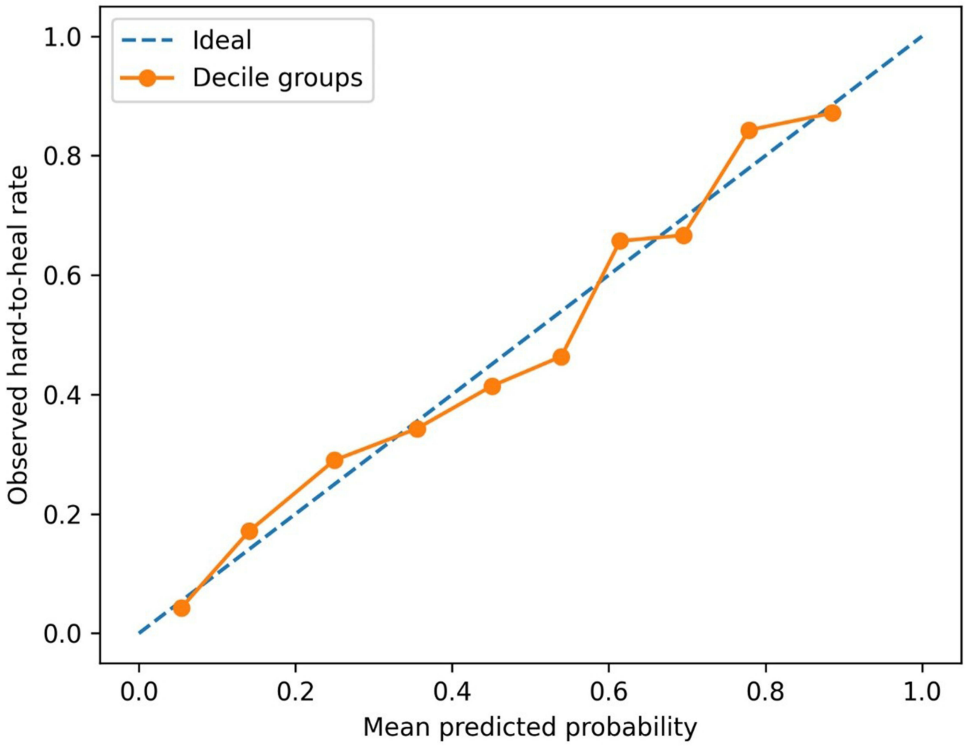

Figure 4 Calibration plot (deciles of predicted risk). Calibration plot comparing mean predicted probability vs observed 12-week hart-to-heal rate within deciles of predicted risk. The dashed diagonal line indicates perfect calibration. Calibration slope was 0.94 and intercept was −0.03.

the IVM model provided net benefit over treat-all and treat-none strategies across clinically relevant threshold probabilities (approximately 0.25–0.70), supporting potential utility for early risk-informed triage (Figure 5). Complete-case sensitivity analysis (n=642) yielded similar discrimination (AUC 0.79, 95% CI 0.76–0.83), and phenotype effect estimates remained directionally consistent.

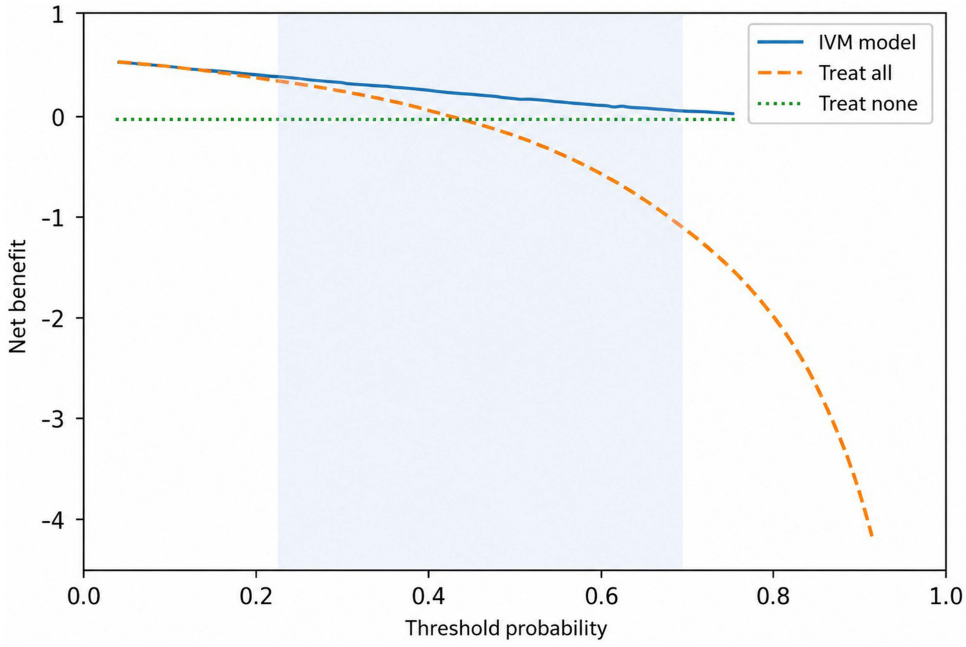

Figure 5 Decision curve analysis (DCA). DCA evaluating clinical utility of the IVM model across threshold probabilities. Net benefit is shown for the IVM model compared with treat-all and treat-none strategies. The shaded region denotes the prespecified clinically relevant threshold probability range of approximately 0.25–0.70.

https://doi.org/10.2147/CIA.S604608

Risk Stratification

When predicted risks were categorized into three clinically interpretable strata (low <0.25; intermediate 0.25–0.70; high >0.70), observed event rates demonstrated clear separation and remained consistent with the intended risk gradient, with 19.7% (50/254; 95% CI 15.3–25.0) hard-to-heal events in the low-risk stratum, 48.8% (137/281; 95% CI 43.0–54.6) in the intermediate-risk stratum, and 89.5% (145/162; 95% CI 83.8–93.3) in the high-risk stratum (Table 4B).

Discussion

Our principal findings indicate that low-energy trauma-initiated foot wounds in older adults are not a homogeneous entity but instead cluster into distinct, clinically interpretable host susceptibility phenotypes spanning vascular impairment, immunoinflammatory burden, and metabolic–nutritional reserve, with markedly different 12-week prognoses. In a cohort of 697 patients (median age 74 years), nearly half developed a hard-to-heal outcome by 12 weeks (47.6%), and latent class analysis identified four phenotypes with a strong risk gradient, ranging from a relatively resilient group with low event rates (18.2%) to ischemia-dominant, metabolic–inflammatory, and renal-hypoalbuminemia groups with substantially higher event rates (49.1%–62.8%) and large adjusted effect sizes versus resilient (adjusted ORs 3.8–6.1). Building on these phenotype insights, the six-variable IVM score provided robust, internally validated prediction of 12-week hard-to-heal outcomes, and yielded clinically meaningful separation into low-, intermediate-, and high-risk strata with observed event rates of 19.7%, 48.8%, and 89.5%, respectively. These findings support the premise that early risk stratification in this geriatric trauma population could be used to guide timely escalation of perfusion assessment and multidisciplinary care.

The metabolic–inflammatory phenotype plausibly reflects an immunometabolic imbalance in which hyperglycemia/diabetes mellitus amplifies a non-resolving inflammatory program. This pattern may reflect stalled inflammation driven by neutrophil and macrophage dysfunction, impaired resolution, and sustained cytokine signaling that collectively compromise angiogenesis and repair.[17,18] The observation that our IVM score retained both ln(CRP) and NLR supports framing these markers as pragmatic proxies of systemic inflammation and immune balance, where CRP indicates acute-phase inflammatory burden and NLR reflects a stress-associated shift toward innate effector predominance relative to adaptive cellular reserve. Importantly, NLR has been linked to healing trajectories in DFU cohorts, supporting its use as a clinically accessible immune-balance surrogate.[19] The renal-hypoalbuminemia phenotype aligns with the geroscience framework of inflammaging and immunosenescence, where older adults, particularly those with reduced organ reserve, exhibit chronic low-grade inflammation alongside impaired adaptive immune competence, increasing susceptibility to infection and limiting regenerative capacity.[20,21] In this context, low albumin is better interpreted as an integrated signal of inflammation/catabolism rather than nutrition alone, and CKD-related immune dysfunction provides an additional mechanistic bridge between reduced eGFR/CKD and impaired host defense in chronic wounds.[22,23] Finally, the ischemia-dominant phenotype had the highest risk, consistent with the concept that tissue hypoperfusion/hypoxia constrains effective immune-cell recruitment and antimicrobial delivery while sustaining a pro-inflammatory wound milieu. Hypoxia-inducible factor biology and hypoxia-response pathways provide a mechanistic lens for how ischemic microenvironments can perpetuate inflammation and impair coordinated repair.[24]

Most prognostic frameworks for non-healing and limb-threatening outcomes were derived from diabetic foot ulcer or broadly mixed-etiology chronic wound cohorts, whereas our cohort was deliberately focused on older adults with low-energy trauma-initiated foot wounds below the malleoli, a starting event that is common in geriatric practice but underrepresented in DFU-centric model development. A key implication is that tools optimized for DFU populations may be imperfectly transportable because DFU often begins with neuropathy and repetitive pressure, and DFU comparative studies commonly rely on standardized DFU severity descriptors (eg., SINBAD) intended for cross-site benchmarking rather than for capturing geriatric trauma-associated host vulnerability.[25] On the other hand, mixed-etiology prediction efforts, such as large EMR-based models predicting 12-week wound healing, demonstrate the feasibility of using routine clinical variables at scale but inherently blend arterial, venous, pressure, diabetic, and other ulcer types, which can dilute mechanistic specificity for any one clinical scenario.[6] Our phenotype-first design may add values by embedding an inflammation–vascular–metabolic host interpretation into a targeted geriatric trauma cohort and

translating it into an interpretable six-variable IVM score with good internal validity. Additionally, anchoring the vascular component in structured perfusion testing and cautious interpretation is consistent with contemporary PAD/CLTI guidance that emphasizes objective testing and recognizes the limitations of ABI in noncompressible vessels, reinforcing the biological plausibility of ischemia as a dominant driver in a subset of these wounds.[12,26,27]

Clinically, the combination of phenotypes and three-tier IVM risk stratification suggests a practical score-guided standardized pathway for older adults with trauma-initiated foot wounds, where the goal is not simply to predict non-healing but to trigger time-sensitive, mechanism-aligned actions. In our cohort, observed 12-week hard-to-heal rates separated sharply into low, intermediate, and high risk, and decision-curve analysis supported net benefit over treat-all /treat-none across threshold probabilities, which is a clinically plausible range for escalation decisions.

For patients assigned to high risk or the ischemia-dominant phenotype, the pathway should prioritize completion of perfusion assessment and early vascular evaluation, consistent with PAD/CLTI guidance that promotes objective hemodynamic assessment to estimate healing likelihood and guide consideration of revascularization in appropriate contexts.[26,27] For metabolic–inflammatory high-risk patients, a standardized approach would emphasize prompt glycemic management (including recognition of stress hyperglycemia) consistent with Endocrine Society guidance for hospitalized non-critical care settings, alongside systematic infection screening and treatment escalation guided by diabetes-related foot infection principles for patients with diabetes.[28,29] For renal-hypoalbuminemia high-risk patients, pathway elements should include early frailty and nutrition assessment and proactive management of CKD-related vulnerability, which may improve tolerance of wound-directed interventions.[22,23] Finally, because successful limb preservation typically requires coordination across vascular care, infection management, glucose control, wound debridement/offloading, and nutrition, our proposed pathway is explicitly multidisciplinary. This is consistent with systematic evidence in DFU care showing that multidisciplinary team models and referral algorithms are associated with reduced major amputation rates and improved outcomes.[30]

Important limitations should be acknowledged. The retrospective single-center design introduces potential selection bias and limits transportability. The IVM model was internally validated only and not externally validated; therefore, calibration and decision thresholds may not transport to other institutions or care pathways. Baseline laboratory values were captured within 48 hours and may partly reflect acute presentation severity and time-from-injury effects, which were not uniformly recorded. Formal frailty assessments were not available in routine documentation; phenotype labels therefore emphasize observed biomarker/renal patterns rather than unmeasured geriatric constructs. Perfusion testing was non-uniform (ABI, Doppler, toe-based measures), which may cause measurement heterogeneity and potential misclassification, particularly for the category that includes noncompressible ABI, which is a measurement limitation rather than a direct ischemia severity indicator. Standardized CLTI (eg., WIfI) and infection severity grading were not consistently documented, so infection was modeled as a binary variable. Similarly, wound severity variables were limited to routinely documented wound area and clinical infection, without standardized recording of wound depth, tissue-loss grade, neuropathy, or offloading adherence. Unmeasured confounding (eg., neuropathy status, detailed wound depth/tissue loss, adherence to offloading, and socioeconomic factors) and between-patient variability in treatment pathways could influence observed associations; and outcome ascertainment based on documentation may introduce misclassification, particularly for healing timing and drainage status at 12 weeks. Future work should prioritize external validation in multicenter cohorts across different regions and care settings to test calibration transportability and refine thresholds. Prospective studies should incorporate standardized microcirculation assessment and standardized infection grading to directly connect host states with repair trajectories, and an impact evaluation is needed to determine whether a score-guided standardized pathway can causally improve healing outcomes compared with usual care.

Conclusion

In conclusion, our findings suggest that low-energy trauma-initiated foot wounds in older adults are best understood through a host-centered framework rather than as a uniform wound entity. The six-variable IVM score showed internally validated discrimination and calibration for 12-week hard-to-heal outcomes and produced clinically meaningful risk strata, which may help structure early triage in the future validation studies. However, routine clinical use should await

external validation across diverse settings and prospective evaluation of whether a score-guided pathway improves healing compared with usual care.

Data Sharing Statement

Data sets generated during the current study are available from the corresponding author on reasonable request.

Ethics Approval and Consent to Participate

This study was conducted in accordance with the Declaration of Helsinki. The protocol was reviewed and approved by the Ethics Committee of the Qingdao Eighth People's Hospital (QBYLLKY2026012), which waived the requirement for informed consent because this was a retrospective analysis of de-identified routinely collected data and posed no more than minimal risk to participants. All data were anonymized prior to analysis.

Funding

This work was funded by the project entitled "Effects of sustained-release VEGF combined with stem cells in artificial dermis for wound repair" (Grant No. 202304100990).

Disclosure

The authors have no conflicts of interest to declare.

References

1. Carter MJ, DaVanzo J, Haught R. et al. Chronic wound prevalence and the associated cost of treatment in Medicare beneficiaries: changes between 2014 and 2019. *J Med Econ*. 2023;26(1):894–901. doi:10.1080/13696998.2023.2232256
2. Kakara R, Bergen G, Burns E, Stevens M. Nonfatal and fatal falls among adults aged ≥65 years—United States, 2020–2021. *MMWR Morb Mortal Wkly Rep*. 2023;72(35):938–943. doi:10.15585/mmwr.mm7235a1
3. Khalid KA, Nawi AFM, Zulkifli N, Barkat MA, Hadi H. Aging and wound healing of the skin: a review of clinical and pathophysiological hallmarks. *Life*. 2022;12(12):2142. doi:10.3390/life12122142
4. Fife CE, Eckert KA, Carter MJ. Publicly reported wound healing rates: the fantasy and the reality. *Adv Wound Care*. 2018;7(3):77–94. doi:10.1089/wound.2017.0743
5. Xie XR, Yu MF, Xu R, Liu Y, Zhang J. From ulcer to amputation: a systematic review of prognostic models for diabetic foot ulcer amputation. *Risk Manag Healthc Policy*. 2025;18:3099–3111. doi:10.2147/RMHP.S542262
6. Cho SK, Mattke S, Gordon H, Sheridan M, Ennis W. Development of a model to predict healing of chronic wounds within 12 weeks. *Adv Wound Care*. 2020;9(9):516–524. doi:10.1089/wound.2019.1091
7. Gurtner GC, Werner S, Barrandon Y, Longaker MT. Wound repair and regeneration. *Nature*. 2008;453(7193):314–321. doi:10.1038/nature07039
8. Eming SA, Martin P, Tomic-Canic M. Wound repair and regeneration: mechanisms, signaling, and translation. *Sci Transl Med*. 2014;6(265):265sr6. doi:10.1126/scitranslmed.3009337
9. Martin P, Nunan R. Cellular and molecular mechanisms of repair in acute and chronic wound healing. *Br J Dermatol*. 2015;173(2):370–378. doi:10.1111/bjd.13954
10. Rodrigues M, Kosaric N, Bonham CA, Gurtner GC. Wound healing: a cellular perspective. *Physiol Rev*. 2019;99(1):665–706. doi:10.1152/physrev.00067.2017
11. Wilkinson HN, Hardman MJ. Wound healing: cellular mechanisms and pathological outcomes. *Open Biol*. 2020;10(9):200223. doi:10.1098/rsob.200223
12. Fitridge R, Chuter V, Mills J, et al. The intersocietal IWGDF, ESVS, SVS guidelines on peripheral artery disease in people with diabetes mellitus and a foot ulcer. *J Vasc Surg*. 2023;78(5):1101–1131. doi:10.1016/j.jvs.2023.07.020
13. Tay WL, Lo ZJ, Hong Q, Yong E, Chandrasekar S, Tan GWL. Toe pressure in predicting diabetic foot ulcer healing: a systematic review and meta-analysis. *Ann Vasc Surg*. 2019;60:371–378. doi:10.1016/j.avsg.2019.04.011
14. Dungan KM, Braithwaite SS, Preiser JC. Stress hyperglycaemia. *Lancet*. 2009;373(9677):1798–1807. doi:10.1016/S0140-6736(09)60553-5
15. Grada A, Phillips TJ. Nutrition and cutaneous wound healing. *Clin Dermatol*. 2022;40(2):103–113. doi:10.1016/j.clindermatol.2021.10.002
16. Syed-Ahmed M, Narayanan M. Immune dysfunction and risk of infection in chronic kidney disease. *Adv Chronic Kidney Dis*. 2019;26(1):8–15. doi:10.1053/j.ackd.2019.01.004
17. Clayton SM, Shafikhani SH, Soulika AM. Macrophage and neutrophil dysfunction in diabetic wounds. *Adv Wound Care*. 2024;13(9):463–484. doi:10.1089/wound.2023.0149
18. Dawi J, Tumanyan K, Tomas K, et al. Diabetic foot ulcers: pathophysiology, immune dysregulation, and emerging therapeutic strategies. *Biomedicines*. 2025;13(5):1076. doi:10.3390/biomedicines13051076
19. Vatankhah N, Jahangiri Y, Landry GJ, et al. Predictive value of neutrophil-to-lymphocyte ratio in diabetic wound healing. *J Vasc Surg*. 2017;65(2):478–483. doi:10.1016/j.jvs.2016.08.108
20. Aiello A, Farzaneh F, Candore G, et al. Immunosenescence and its hallmarks: how to oppose aging strategically? *Front Immunol*. 2019;10:2247. doi:10.3389/fimmu.2019.02247

21. Santoro A, Bientinesi E, Monti D. Immunosenescence and inflammaging in the aging process: age-related diseases or longevity? *Ageing Res Rev*. 2021;71:101422. doi:10.1016/j.arr.2021.101422
22. Soeters PB, Wolfe RR, Shenkin A. Hypoalbuminemia: pathogenesis and clinical significance. *JPEN J Parenter Enteral Nutr*. 2019;43(2):181–193. doi:10.1002/jpen.1451
23. Espi M, Koppe L, Fouque D, Thaunat O. Chronic kidney disease-associated immune dysfunctions: impact of protein-bound uremic retention solutes on immune cells. *Toxins*. 2020;12(5):300. doi:10.3390/toxins12050300
24. Hong WX, Hu MS, Esquivel M, et al. The role of hypoxia-inducible factor in wound healing. *Adv Wound Care*. 2014;3(5):390–399. doi:10.1089/wound.2013.0520
25. Ince P, Abbas ZG, Lutale JK, et al. Use of the SINBAD classification system and score in comparing outcome of foot ulcer management on three continents. *Diabetes Care*. 2008;31(5):964–967. doi:10.2337/dc07-2367
26. Gornik HL, Aronow HD, Goodney PP, et al. 2024 ACC/AHA/AACVPR/APMA/ABC/SCAI/SVM/SVN/SVS/SIR/VESS guideline for the management of lower extremity peripheral artery disease. *J Am Coll Cardiol*. 2024;83(24):2497–2604. doi:10.1016/j.jacc.2024.02.013
27. Conte MS, Bradbury AW, Kolh P, et al. Global vascular guidelines on the management of chronic limb-threatening ischemia. *J Vasc Surg*. 2019;69(6S):3S–125S. doi:10.1016/j.jvs.2019.02.016
28. Senneville É, Albalawi Z, van Asten SA, et al. IWGDF/IDSA guidelines on the diagnosis and treatment of diabetes-related foot infections (IWGDF/IDSA 2023). *Diabetes Metab Res Rev*. 2024;40(3):e3687. doi:10.1002/dmrr.3687
29. Korytkowski MT, Muniyappa R, Antinori-Lent K, et al. Management of hyperglycemia in hospitalized adult patients in non-critical care settings: an Endocrine Society clinical practice guideline. *J Clin Endocrinol Metab*. 2022;107(8):2101–2128. doi:10.1210/clinem/dgac278
30. Musuuza J, Sutherland BL, Kurter S, Balasubramanian P, Bartels CM, Brennan MB. A systematic review of multidisciplinary teams to reduce major amputations for patients with diabetic foot ulcers. *J Vasc Surg*. 2020;71(4):1433–1446. doi:10.1016/j.jvs.2019.08.244